JOURNAL OF CATALYSIS 157, 179–189 (1995)

Promoter Effect of Pd in Hydrogenation of 1,3-Butadiene over Co–Pd Catalysts

A. Sárkány, Z. Zsoldos, Gy. Stefler, J. W. Hightower,* and L. Guczi

*Department of Surface Chemistry and Catalysis, Institute of Isotopes of the Hungarian Academy of Sciences, P.O. Box 77, Budapest, Hungary, H-1525; *Department of Chemical Engineering, MS-362, Rice University, Houston, Texas 77005-1892*

Received August 9, 1994; revised June 23, 1995; accepted July 12, 1995

Addition of a second metal or metal oxide often improves the selectivity of a supported catalyst for the hydrogenation of 1,3-butadiene impurities in commercial *n*-butene streams. This research has explored the effect of adding Pd to cobalt supported on alumina. Catalysts containing 5 wt% Co and varying amounts (0.1 to 1.0 wt%) of Pd were prepared and characterized by X-ray diffraction, X-ray photoelectron spectroscopy, chemisorption of CO and H_2, and temperature-programmed reduction after having been subjected to a variety of carefully controlled pretreatments. Activities and product selectivities were tested for hydrogenation of pure 1,3-butadiene and butadiene in a mixture with 1-butene at room temperature. The presence of Pd increased the reducibility of the Co, and separate aluminate, Co, and Pd–Co bimetallic surface phases were identified following various pretreatments. Increasing the Co/Pd ratio decreased the formation of *n*-butane at room temperature relative to the rate of butadiene conversion, although the improved selectivity was achieved at the expense of increased olefin isomerization and deactivation due to accumulation of carbonaceous residues on the surface. It was not possible to determine unequivocally whether the observed modifications were due to electronic effects or selective poisoning of the separate Co sites.

INTRODUCTION

Selective hydrogenation of dienes, alkynes, and other highly unsaturated hydrocarbons is of great industrial importance (1–3). 1,3-Butadiene is almost always present as a major impurity in C_4 alkenes produced by steam cracking of naphtha or by catalytic cracking of heavier hydrocarbons. For many industrial applications the butadiene content must be considerably reduced without significant losses of butenes either by saturation or by isomerization. 2-Butenes are utilized for alkylation or for production of methyl ethyl ketone (MEK), while 1-butene is used as a comonomer in the production of linear low-density polyethylene polymer. Hydrogenation of C_4 cuts is generally performed in the liquid phase in the presence of Pd supported on α-alumina. Some disadvantages of gas-phase hydrogenation are rapid poisoning of the catalyst and high exothermicity of the reaction, which causes problems in heat and mass transfer and complicates process control.

Both the hydrogen availability and the strength of diene (or alkyne) complexation can be modified by the addition of a second metal, thereby improving the selectivity of alkene formation and extending the lifetime of the catalyst. The bimetallic catalysts allow a larger degree of freedom to tune the reaction sites for optimum activity and selectivity (13, 14). In fact, investigations with Pb–Pd (4–9), Cr–Pd (10), Sn–Pd, Ge–Pd, Bi–Pd (11), and Cu–Pd (12) catalysts have confirmed that for several substrates the bimetallic samples are superior to Pd/Al_2O_3 in selective hydrogenations.

Co has found widespread industrial application as the primary active component of hydrogenation and hydrotreating catalysts. Recent results (15, 16) have confirmed the beneficial effect of Pt or Ru on reduction of Co in hydrogenation of CO to produce middle distillates. Work in our laboratory has shown that Pt and Pt–Co bimetallic particles as well as Co surface phases can be formed with different pretreatments (17–19). Systematic investigations of 1,3-butadiene hydrogenation over Co (20–22) have indicated high selectivity for *n*-butene formation but rather low hydrogenation activity. The rate of *n*-butene isomerization significantly exceeds the rate of hydrogenation, but only after most of the butadiene has been depleted. Selectivity for specific *n*-butenes has been observed to depend strongly on poisoning. For example, a dominance of 1-butene is formed on clean Co surfaces, whereas *trans*-2-butene is the primary reaction product on sulfur- or chlorine-modified surfaces.

The present paper deals with hydrogenation of 1,3-butadiene on Pd-modified Co/Al_2O_3 catalysts. Co alone on Al_2O_3 (23–25) forms both surface spinel and oxide phases,

[1] To whom correspondence should be addressed at: Department of Chemical Engineering, Rice University, MS-362, 6100 South Main, Houston, TX 77005-1892. Fax: 713/285-5478. E-mail: jhigh@owlnet.rice.edu.

0021-9517/95 $12.00

but only the latter can be reduced below 673 K. This low reducibility of Co ions is one of the factors that limit hydrogenation activity. Furthermore, upon hydrogen treatment Pd atoms in bimetallic samples are likely to segregate on the surface of Co, thereby providing an increased concentration of surface hydrogen.

Preparation of bimetallic Co–Pd catalysts also raises the question whether cobalt acts as a structural promoter affecting only the dispersion of Pd particles or Pd–Co mixed sites participate collectively in activating the hydrogen. The effect of surface sites on the complexation strength of diene and alkene over Co–Pd catalysts is another question to be answered. In this work 5 wt% Co/Al_2O_3 was modified with Pd (Pd/Co atomic ratio = 0.01, 0.05, and 0.1) and the effect of Pd on the reducibility and product selectivity was tested.

EXPERIMENTAL

Catalyst Preparation

A precursor of 5 wt% Co/Al_2O_3 catalyst was prepared by incipient wetness with a methanol solution of $Co(NO_3)_2 \cdot 6H_2O$. The support (Condea SB, high-purity boehmite) was air-treated at 823 K for 4 h prior to impregnation to transform it into γ-alumina with a BET surface area of 192 m^2/g. The mesopore size distribution calculated from the nitrogen isotherm indicated a maximum at 6.5 nm diameter, and the cumulative pore volume was 0.50 cm^3/g. Impregnation of the support with 5 wt% Co and subsequent calcination at 723 K for 2 h decreased these numbers only slightly, with the new values being 185 m^2/g, 5.2 nm, and 0.37 cm^3/g, respectively.

After the 5 wt% Co/Al_2O_3 precursor was dried for 16 h at 401 K, aliquots were impregnated in a second step at 353 K with various amounts of $Pd(NH_3)_2(NO_2)_2$ complex dissolved in solutions of ammonia and methanol (pH 9.7–10.2) to prepare catalysts with compositions 0.1 wt% Pd–5 wt% Co, 0.5 wt% Pd–5 wt% Co, and 1 wt% Pd–5 wt% Co; the atomic Pd/Co ratios are 0.01, 0.05, and 0.1, respectively. Upon impregnation with the Pd complex the original pink color of the sample turned dark, which indicates the oxidation of Co^{2+} to Co^{3+} in the basic medium. In the absence of the Pd complex, i.e., when only base was added, the oxidation of Co^{2+} in air was slower. Catalysts of 1 wt% Pd/Al_2O_3 and 0.1 wt% Pd/Al_2O_3 were also prepared and treated in a manner similar to the Co-containing samples. Catalyst precursors were calcined at 473 K, stored in sealed bottles, and subjected to different treatments before reduction. In order to avoid support effects, unsupported bimetallic Pd–Co samples (metallic content of 11.4 and 49.3 at.% Pd) were also prepared from PdO and $Co(OH)_2$ by carefully mixing the constituents. The samples were oxidized at 723 K under O_2 for 15 min and used in temperature-programmed reduction (TPR), XRD, and X-ray photoelectron spectroscopy (XPS) measurements.

Catalyst Characterization

Temperature-programmed reductions were measured in 9.2 vol% H_2 in argon at a flow rate of 43–44 cm^3/min with a temperature ramp rate of 20 K/min starting from room temperature. The same system was used for hydrogen chemisorption measurements. In the latter case frontal chromatography (the partial pressure of hydrogen was 263.4 Pa), desorption tests, and pulse methods were applied (sample volumes were 0.1 and 0.01 cm^3). The pulse method described in detail by Falconer and Schwarz (30) and Lee and Schwartz (31) was used in determining the activation energy of hydrogen adsorption. Thermal desorption tests were also applied to obtain hydrogen chemisorption data. Gases were carefully purified: high-purity H_2 was passed through $Pd–Pt/Al_2O_3$ and 5A molecular sieves, and high-purity argon was contacted with partially reduced Mn^{2+} and 5A molecular sieves before use. CO chemisorption was measured gravimetrically at ambient temperature by means of a Sartorius (Type 4102) microbalance.

CuK_α X-ray powder diffractograms were recorded with a Guinier camera equipped with a curved quartz monochromator.

X-ray photoelectron spectroscopic measurements were carried out in a Kratos ES-300 ESCA instrument working in fixed retarding ratio (FRR) mode. Spectra were generated by AlK_α X rays ($h\nu$ = 1486.67 eV, 150 W). During computer-controlled spectra recording, the pressure in the analyzing chamber did not exceed 10^{-6} Pa. After the first *ex situ* calcination at 723 K the powder samples were pressed into a copper grid and then mounted onto the tip of the sample holder rod. Further sample treatments were carried out in an atmospheric chamber attached directly to the ESCA machine, thereby preventing air exposure between reduction pretreatments and XPS measurements. The Fermi level of the fully reduced powder mixture was used as a binding energy (BE) reference.

The catalysts were tested by gas phase hydrogenation of 1,3-butadiene in a static recirculation system (volume 187 cm^3). Most of the hydrogenations were performed with $BD:H_2$ = 1:2 ratios unless otherwise stated. Products were separated by GLC using a 20% BMEA column at 303 K. As in earlier publications (26, 27), product selectivities were calculated as the cumulative moles of a product formed divided by the total moles of butadiene consumed. In order to characterize the performance of these catalysts, activity and selectivity tests were also run with a mixture of 1-butene and 1,3-butadiene (typically 8.9 mol% 1,3-butadiene in 1-butene). Negative selectivity values for 1-butene are observed when the 1-butene concentration during the course of hydrogenation becomes less than the initial concentration.

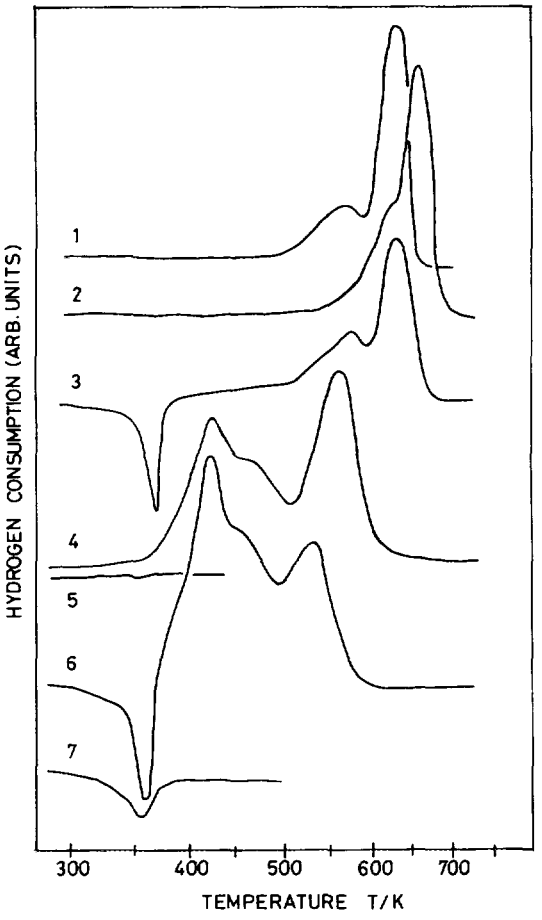

FIG. 1. Temperature-programmed reduction: (1) Co_3O_4; (2) Co_3O_4, previously reduced sample oxidized at 623 K; (3) mechanical mixture of PdO + Co_3O_4, 11.2 at.% Pd; (4) previously reduced sample oxidized at 623 K; (5) repeated TPR with reduced sample (4); (6) mechanical mixture of PdO + Co_3O_4 (with 48 at.% Pd) reduced and oxidized at 623 K prior to TPR; (7) repeated TPR with reduced sample (6).

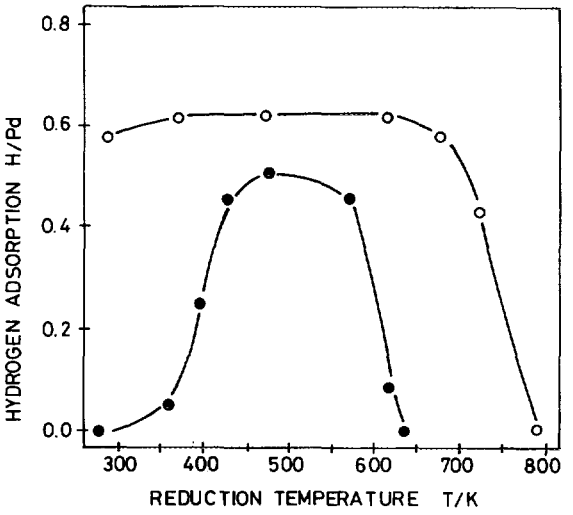

FIG. 2. Hydrogen adsorption as a function of reduction temperature (for conditions see text). Open symbols, mechanical mixture of PdO + Co_3O_4 (11.4 at.% Pd); filled symbols, sample reduced and oxidized at 623 K.

RESULTS

Temperature-Programmed Reduction

Cobalt hydroxide was chosen as a model system with which the supported catalysts could be compared. When $Co(OH)_2$ was treated with O_2 at 723 K, Co_3O_4 was formed, as indicated by the TPR and confirmed also by XRD and XPS. The TPR spectrum in Fig. 1 (curve 1) shows that Co_3O_4 is reduced in two steps: The first peak at 563 K can be assigned to reduction of Co^{3+} to Co^{2+} and the second peak at 623 K to the formation of metallic Co. Treatment of the reduced sample with O_2 at 723 K for 30 min followed by another reduction gave curve 2. The main reduction peak shifted from 600 to 650 K and the first reduction step now appears as a shoulder. As a consequence of sintering, which apparently causes transport limitation of hydrogen into the particles, the two reduction steps could not be separated at the 20 K/min ramp rate.

After a mechanical mixture of PdO and Co_3O_4 (11 at.% of the metal was Pd) had been treated with O_2 at 723 K for 2 h, its reduction profile in curve 3 showed a sharp negative peak at 353 K, which can be attributed to the decomposition of Pd hydride formed in the reduction of PdO under H_2/Ar before the ramp was started at 295 K. The shift of the baseline above 373 K indicates that there was some limited contact between Pd and Co_3O_4 particles. Nevertheless, considering the peak positions, the reduction of Co_3O_4 is hardly affected by Pd. The TPR profile of the sample once reduced and reoxidized at 623 K (curve 4) showed the following features: (i) The peak intensity at 353 K essentially vanishes, which points to the elimination of the hydride phase. The hydride phase can be regenerated, however, by reducing the sample at successively higher temperatures (20 K/min ramp rate up to a given temperature and cooling back to ambient under hydrogen) as shown in Fig. 2. The apparent discrepancy stems from the fact that most of the Pd phase was reduced at a temperature higher than that of the hydride phase decomposition. With the formation of metallic Co the hydride formation is completely suppressed. (ii) Three reduction peaks appear at 423, 473, and 558 K. (iii) An increase in Pd concentration (compare 11.4 and 49.4 at.% Pd–Co samples, curves 4 and 6) increases the relative intensity of the first reduction peak. In the fully reduced 49.4 at.% Pd sample, formation of the hydride phase is suppressed but to a smaller extent than with the 11 at.% Pd–Co sample (curves 5 and 7).

All supported Pd–Co/Al_2O_3 samples were O_2 treated at a maximum temperature of 623 K for 30 min in order to limit surface spinel formation. The reduction spectra are presented in Fig. 3. The amounts of consumed hydro-

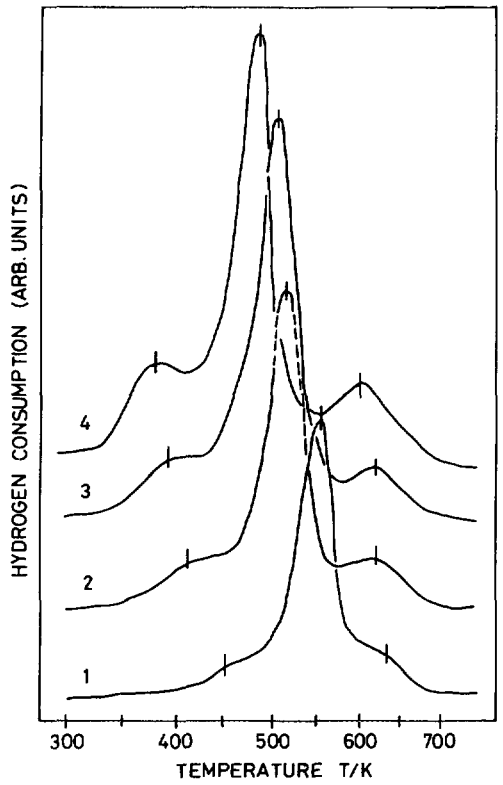

FIG. 3. TPR of Pd–Co/Al_2O_3 samples calcined under O_2 at 623 K: (1) 5 wt% Co/Al_2O_3; (2) 0.1 wt% Pd–5 wt% Co/Al_2O_3; (3) 0.5 wt% Pd–5 wt% Co/Al_2O_3; and (4) 1 wt% Pd–5 wt% Co/Al_2O_3.

gen are collected in Table 1. In the reduction of the 5 wt% Co/Al_2O_3 sample (curve 1), the main reduction peak appears at 546 K together with small shoulders at 453 and 623 K. In the presence of Pd, the amount of consumed hydrogen increases and the reduction peaks shift gradually to lower temperatures (curves 2–4).

Oxidation of the precursors at 723 K for 4 h decreases the amount of hydrogen consumed (Table 1), and the reduction peaks become broader and are not well resolved (Fig. 4). It is worth noting that the intensity of the first reduction peak at 373–393 K is not affected significantly by repeated oxidation–reduction treatments at 623 or 723 K, and its intensity increases with Pd concentration. For the 1% Pd/Al_2O_3, the formation of the hydride phase could be clearly detected by TPD on cooling the sample from 473 K under 9.2 vol% H_2. The hydride phase decomposed with a peak minimum at 360 K. With the Co–Pd/Al_2O_3 samples neither formation nor decomposition of the hydride phase was observed, nor did the hydride phase appear after reduction at 573 or 723 K.

Moreover, the amount of hydrogen consumed for the 1 wt% Pd-5 wt% Co/Al_2O_3 sample is generally higher than that required for reduction of Pd. This is probably due to simultaneous reduction of a small amount of Co^{3+} to Co^{2+}. Even with our 5 wt% Co/Al_2O_3 a small reduction peak can always be seen at 373–423 K, which probably represents the $Co^{3+} \rightarrow Co^{2+}$ transformation.

TABLE 1

Reduction and Oxidation of Pd–Co/Al_2O_3 Catalysts

	I				II				
	H_2[a]		O_2[b]		H_2[a]		O_2[b]		
Catalyst	Co–Pd	Co	Co–Pd	Co	Co–Pd	Co	Co–Pd	Co	R[c]
5Co–1Pd	814	720	267	221	486	392	283	198	35
5Co–0.5Pd	736	689	228	205	430	383	221	192	34
5Co–0.1Pd	639	629	182	178	354	344	177	172	30
5Co	439	439	61	61	106	106	44	44	8

Note. I, O_2 treatment at 623 K; II, O_2 treatment at 723 K.
[a] H_2 consumption measured between 298 and 733 K (μmol/g_{cat}).
[b] O_2 uptake measured at 723 K (μmol/g_{gat}).
[c] Degree of reduction to Co^0 (%) assuming reduction of Co_3O_4.

Chemisorption Measurements

As shown in Table 2 the total amount of CO adsorbed on samples reduced at 723 K for 4 h was measured gravi-

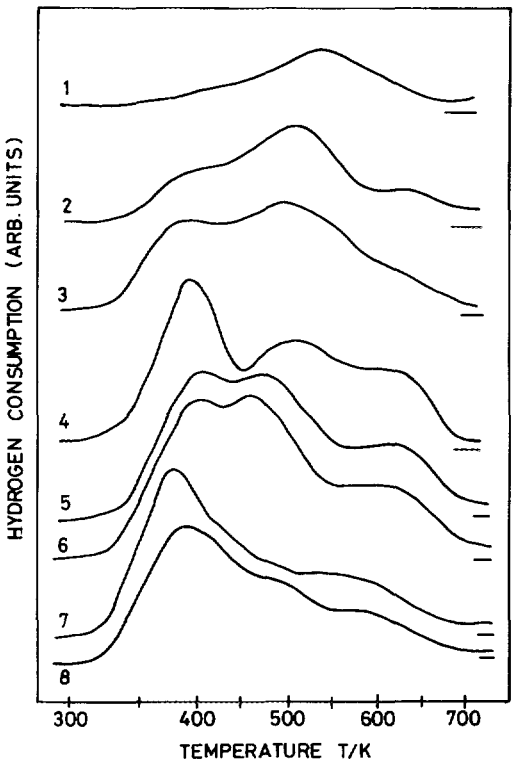

FIG. 4. TPR of Pd–Co/Al_2O_3 samples calcined at 723 K: (1) 5 Co; (2) 0.1Pd5Co; (3) 0.5Pd5Co; (4) 1Pd5Co. TPR with 1Pd5Co sample: (5) reduced at 724 K and then O_2 treated at 623 K; (6) reduced up to 700 K (curve 4), then O_2 treated at 623 K; (7) O_2 treated at 823 K prior to reduction; (8) reduced at 773 K then O_2 treated at 773 K.

TABLE 2

CO Chemisorption at 298 K and Hydrogen Uptake from Desorption Measurements (μmol/g_{cat})

Catalyst	CO(tot)	CO(irr)	CO(rev)/CO(irr)	H_2
$1Pd/Al_2O_3$	35.2	29.5	0.19	17.6
$0.1Pd/Al_2O_3$	n.m.[a]	1.3	—	0.8
$1Pd–5Co/Al_2O_3$	73.7	57.8	0.27	66.7
$0.5Pd–5Co/Al_2O_3$	56.8	45.1	0.26	43.2
$0.1Pd–5Co/Al_2O_3$	46.1	36.7	0.25	20.3
$5Co/Al_2O_3$	43.3	25.8	0.68	5.2

[a] Not measured.

metrically at 273 K under 133 Pa CO pressure equilibrated for 5 min (column 2). After evacuation at 10^{-5} Pa for 15 min to remove weakly bound CO, the irreversibly bound CO was recorded (column 3). This effect is most pronounced with pure Co and catalysts with low Pd loading, which indicates the formation of surface Co-subcarbonyls.

Figure 5 shows the chemisorption of hydrogen measured by frontal chromatography in the temperature range 273–510 K. After each catalyst had been reduced at 723 K for 8 h under hydrogen, adsorbed hydrogen was removed by Ar flowing at 623 K for 15 min and the sample was cooled to the temperature at which chemisorption from 0.26 vol% H_2/Ar (263.4 Pa H_2) was to be measured. These experiments indicated activated adsorption of hydrogen (28, 29). For the 5 wt% Co/Al_2O_3 sample the maximum hydrogen uptake occurred at about 450 K. The presence of Pd increased the amount of adsorbed hydrogen but decreased the temperature at which the maximum was observed on the Pd–Co samples.

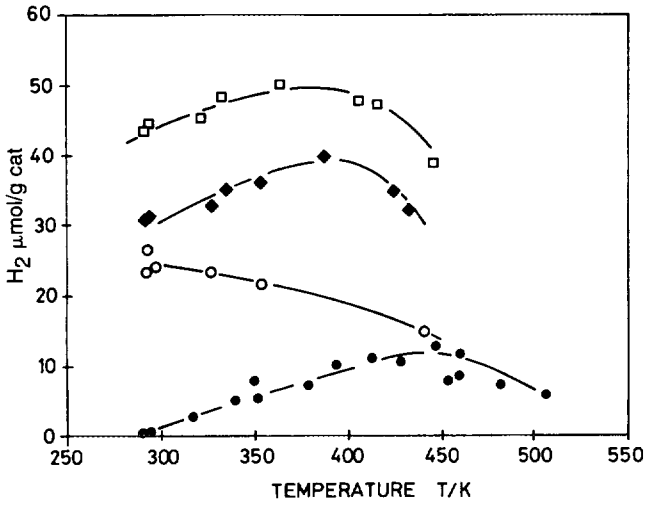

FIG. 5. Hydrogen adsorption as a function of adsorption temperature. (●) 5Co; (○) 1Pd; (◆) 0.5Pd5Co; and (□) 1Pd5Co.

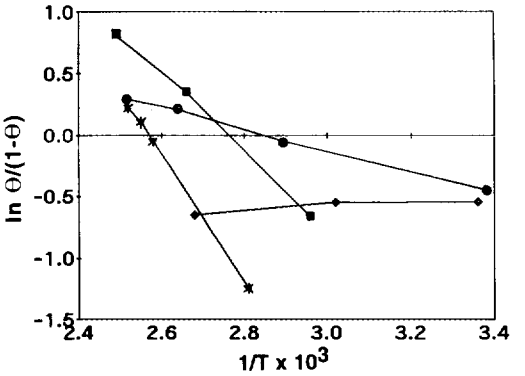

FIG. 6. Adsorption energy of hydrogen chemisorption. (●) 1Pd5Co; (◆) 1Pd; (■) 0.1Pd5Co; and (*) 5Co.

The ratios of CO chemisorption to strongly bound hydrogen, CO/H at 298 K, were 1.79, 0.98, 0.72, 0.72, and 0.7 for the 5Co, 0.1Pd–5Co, 0.5Pd–5Co, 1Pd–5Co, and $1Pd/Al_2O_3$ samples, respectively. TPD supplemented the hydrogen chemisorption presented in Table 2. The catalysts were reduced under H_2 at 673 K for 4 h; then H_2 was replaced with 0.12 vol% H_2/Ar and cooled to 273 K. The samples were purged with Ar and TPD measurements were carried out starting at 573 K.

Using the method of Schwartz and co-workers (see Refs. 30, 31) the activation energy of adsorption (E_a) was determined by adding pulses of H_2 in an argon stream and measuring the adsorbed amount. The slope of $Q/(1 - Q)$ versus flow rate of argon was close to -1, indicating sec-

TABLE 3

XPS Data for the PdO + $Co(OH)_2$ Mixture (11.4 at.% Pd) after Different Successive Pretreatments

No.	Treatment T (K)	Treatment Time (min)	BE (eV) $Pd3d_{5/2}$	BE (eV) $Co2_{3/2}$	Intensity ratio $Pd3d/Co2p$	Surface phases
1	$723/O_2$	15	336.7	779.5	0.45	PdO_x, Co_3O_4
2	$373/H_2$	1	335.0	779.5	0.53	Pd, Co_3O_4
3	$673/H_2$	20	335.1	777.8	0.87	Pd, Co
4	$723/H_2$	120	335.1	777.6	1.00	Pd, Co
5	$723/O_2$	60	336.7	779.5	0.21	PdO_x, Co_3O_4
6	$373/H_2$	[a]	335.1	779.5	0.26	Pd, Co_3O_4
7	$423/H_2$	[a]	335.1	779.7	0.22	Pd, Co_3O_4
8	$468/H_2$	[a]	335.1	779.7	0.19	Pd, CoO
9	$675/H_2$	[a]	335.1	777.6	0.62	Pd, Co
10	$723/O_2$	20	336.8	779.5	0.08	PdO_x, Co_3O_4
11	$295/H_2$	10	336.8	779.9	0.08	PdO_x, Co_3O_4
12	$334/H_2$	[a]	335.1	779.8	0.10	Pd, Co_3O_4
			336.9			PdO_x

[a] The sample was heated from ambient at 20 K/min to the temperature given in column 2. Thereafter it was cooled to ambient.

TABLE 4

Hydrogenation of 1,3-Butadiene at 298 K

T (K)	t (min)	Initial % selectivities: n-Butane	Initial % selectivities: 1-Butene	*trans/cis* ratio	$R \times 10^{5a}$
		5 wt% Co/Al_2O_3			
573	30	n.o.	71.9	1.73	0.03
625	30	0.88	70.0	1.94	0.16
675	30	0.98	69.8	1.86	0.31
723	30	1.33	70.6	1.74	0.39
723	120	3.21	67.9	1.69	0.33
723	320	2.12	66.8	1.69	0.28
		0.1Pd–5Co/Al_2O_3			
298	30	n.o.	62.3	4.63	0.01
298	60	n.o.	60.9	4.51	0.02
326	35	n.o.	60.6	3.31	0.03
373	33	n.o.	59.8	3.02	0.08
517	35	n.o.	59.3	2.54	0.19
623	32	0.02	58.2	2.42	0.23
725	33	0.55	57.6	2.47	0.49
728	323	0.25	57.7	2.39	0.83
		1Pd–5Co/Al_2O_3			
298	35	n.o.	63.2	5.55	0.56
330	32	n.o.	61.1	4.72	1.44
431	55	n.o.	58.8	3.21	2.26
480	34	n.o.	56.5	2.98	2.71
528	33	0.01	56.3	2.87	3.17
723	33	0.88	55.5	2.85	7.15
723	246	2.13	56.3	2.77	9.03
		1Pd/Al_2O_3			
323	32	0.04	53.2	6.81	3.63
536	28	0.16	56.6	6.77	4.44
6.74	189	0.11	53.2	6.80	4.11
723	315	0.08	52.2	6.51	4.06

Note. Catalysts pretreated with O_2 at 723 K, reduced with a 20 K/min ramp rate, and cooled under H_2 to 298 K. Columns 1 and 2 give the maximum reduction temperature and the time held at that temperature. $H_2/BD = 2$.

[a] Initial rate of 1,3-butadiene consumption (mols · g_{cat}).

ond-order adsorption of hydrogen. The activation energies of adsorption determined in the temperature range 273–493 K are 7.1, 25.8, and 41.6 kJ/mol for 1Pd–5Co, 0.1Pd–5Co, and 5 Co/Al_2O_3 samples, respectively (Fig. 6). The E_a values indicate a decrease in the energy of H_2 activation with increasing Pd content.

X-Ray Photoelectron Spectroscopy

In order to clarify the changes observed by TPR and XRD after different treatments, the reduction–oxidation processes described for the unsupported PdO + $Co(OH)_2$ sample (11.4 at.% Pd) were followed by X-ray photoelectron spectroscopy. The results are summarized in Table 3.

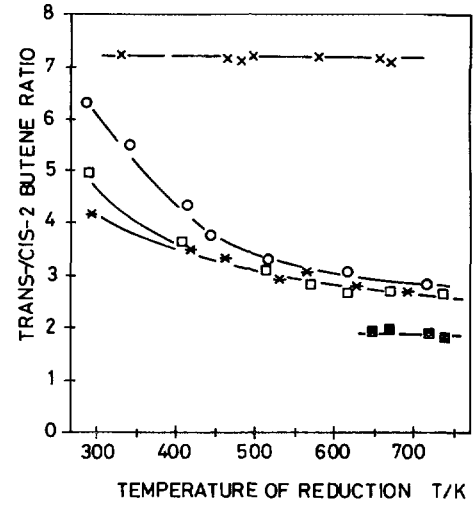

FIG. 7. *Trans/cis*-2-butene ratios formed from 1,3-butadiene at 298 K as a function of reduction temperature (treatment described in text). (×) 0.1Pd; (○) 1Pd5Co; (□) 0.5Pd5Co; and (*) 0.1Pd5Co.

Following initial oxidation, the first sequence of reduction (rows 2–5 in Table 3) confirms that originally Pd is in an oxidized state (Pd3$d_{5/2}$ in PdO is 336.2 eV BE) and the Co phase is present as Co_3O_4. After the first reduction at 373 K, Pd^0 and Co_3O_4 were found, in agreement with the assignment of the last doublet of the TPR curve (Fig. 1, curve 3).

Insight into the reduction steps of the reoxidized sample (Fig. 1, curve 4) is given by the XPS results in rows 6–9 in Table 3. Reduction at 373 K (row 6) indicated formation of Pd^0. Formation of CoO could also be detected at 468 K (row 8). The sample was reoxidized again (row 10), and the reducibility of PdO was tested at 295 and 334 K (rows 10–12 in Table 3). Reduction at 295 K for 10 min did not result in the formation of Pd^0, but Pd^0 did appear at 334

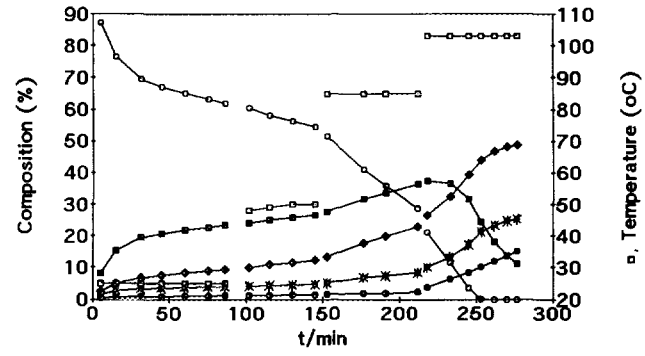

FIG. 8. Hydrogenation of 1,3-butadiene on 5 wt% Co/Al_2O_3 (1.33 kPa BD and 5.32 kPa H_2; temperature gradually increased to compensate for poisoning). (○) 1,3-butadiene; (■) 1-butene; (◆) *trans*-2-butene; (*) *cis*-2-butene; (●) *n*-butane; and (□) temperature.

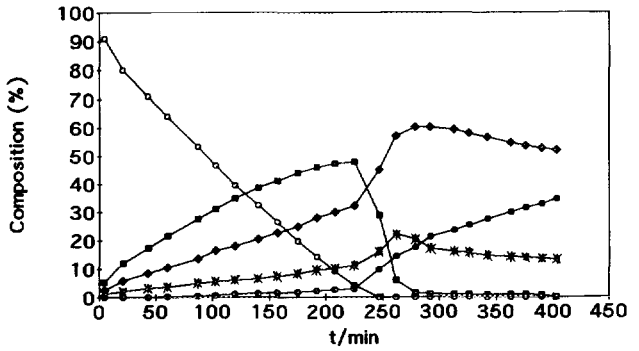

FIG. 9. Hydrogenation of 1,3-butadiene on 0.1 wt% Pd–5 wt% Co/Al_2O_3 at 273 K. For symbols see Fig. 8.

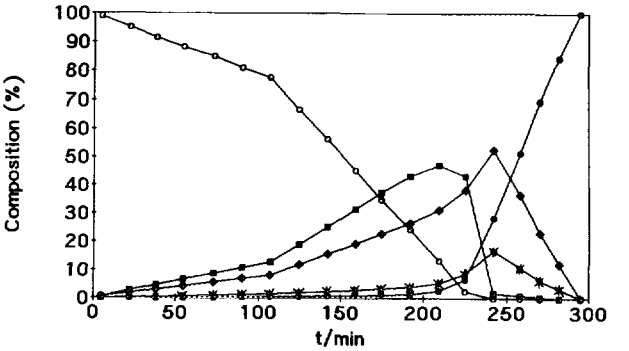

FIG. 10. Hydrogenation of 1,3-butadiene on 1 wt% Pd/Al_2O_3 at 253 and 273 K (1.33 kPa BD and 5.32 kPa H_2). For symbols see Fig. 8.

K. It should be noted that, since the reduction in the pretreatment chamber was performed at atmospheric pressure, the transformations are shifted to lower temperatures than in the TPR runs. Nevertheless, the XPS results confirm that the last two TPR peaks, which are strongly shifted in the presence of Pd, can be attributed to the two-step reduction of Co_3O_4.

Catalytic Measurements

As a chemical probe, hydrogenation of 1,3-butadiene provides further details about the formation of the active surface. In the series of experiments presented in Table 4, after treatment at 723 K under O_2 the catalyst precursor was reduced under 9.5 kPa H_2 at 20 K/min ramp to the temperature given in column 1 (the experimental conditions were close to those applied in the TPR runs). Having been maintained at that temperature for the time given in column 2, the catalyst was cooled back to 298 K and the butadiene reaction rate and product distribution were measured at low (less than 10%) conversions. 1-Butene was the dominant product (>50%) in all cases. Figure 7 shows the *trans/cis*-2-butene ratios presented as a function of the highest reduction temperature. Increasing the reduction temperature decreases the *trans/cis* ratio on the Pd–Co samples but has little effect on the ratios observed on either Pd/Al_2O_3 (6.5–6.8) or Co/Al_2O_3 (1.7–1.9) catalysts. Because of the difficulty in reducing the supported Co catalyst in the absence of Pd, its hydrogenation activity at 298 K appeared only after reduction at temperatures above 573 K.

Typical composition versus time curves are shown in Figs. 8–11. Since with the Co catalyst the initial activity gradually decreased as a result of self-poisoning, the temperature was increased in steps to achieve higher conversions (Fig. 8). The product selectivity at H_2/BD ratio of 4 remains reasonably constant with 1-butene being the dominant product as long as at least 4–8 mol% butadiene is present in the gas phase even at 376 K. At low butadiene concentrations, fast isomerization of *n*-butenes proceeds along with the formation of *n*-butane. In Table 5, $-R_{BD}/R_{nB}$ compares the two states of hydrogenation: the negative slope of butadiene consumption is divided by the slope of the *n*-butane formation at zero BD concentrations. The more selective the catalyst, the larger this number should be. Notice that the ratio increases with decreased Pd concentration in the Pd–Co samples.

Investigations with mixtures of 1-butene and 1,3-butadiene (8.9 mol% butadiene in 1-butene) have revealed further details about the effect of the Co phase (Fig. 12). Under the conditions used (313 K, 118.6 Pa butadiene, 1.21 kPa 1-butene, 151 Pa H_2 balanced to atmospheric pressure with He), all the catalysts gave positive 1-butene selectivities until the butadiene conversion reached at least 85%. However, addition of 5 wt% Co to the sample extended the region of positive 1-butene selectivity to over 90% butadiene conversion for the 1 wt% Pd and to over 99% conversion for the 0.1 wt% Pd catalyst. As expected, the addition of Co also decreased the amount of *n*-butane at comparable butadiene conversions (Fig. 13).

DISCUSSION

The experimental results have confirmed with both Co_3O_4 and 5 wt% Co/Al_2O_3 catalysts that the addition of

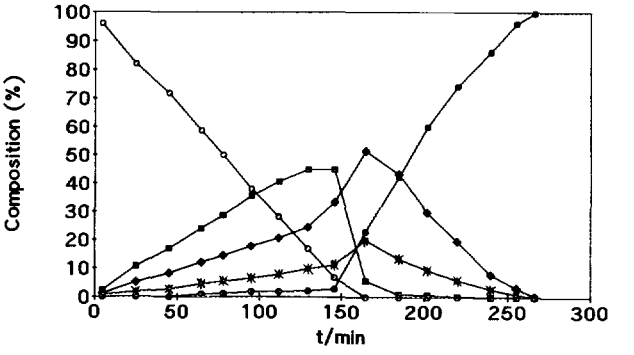

FIG. 11. Hydrogenation of 1,3-butadiene on 1 wt% Pd–5 wt% Co/Al_2O_3 at 273 K. For symbols see Fig. 8.

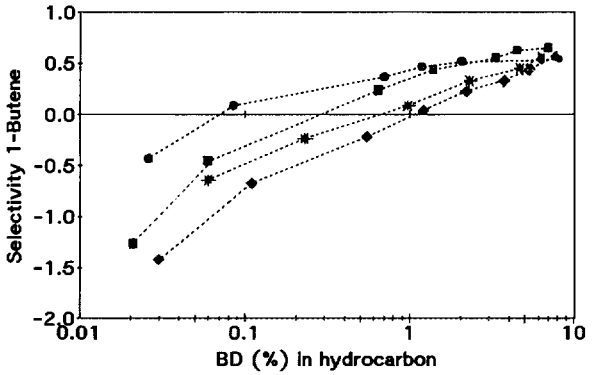

FIG. 12. Selectivity of 1-butene formation in hydrogenation of 8.9 mol% 1,3-butadiene in 1-butene (butadiene + 1-butene, 1.33 kPa; H_2, 135 Pa; T = 293 K). (*) 1Pd, (◆) 1Pd5Co, (●) 0.1 Pd, (■) 0.1Pd5Co.

Pd (1, 5, and 10 at.% Pd) increases the reducibility of Co ions. Unsupported Co_3O_4 (particle size calculated from X-ray broadening is 9.5–11 nm) is reduced in the temperature range of 473–673 K and can be characterized by peak maxima at 553 and 623 K. The reduction of Co_3O_4, in accordance with earlier observations (17), takes place in two consecutive steps: The first peak corresponds to the reduction of Co^{3+} to Co^{2+} and the second to the formation of metallic Co. This conclusion is supported by the peak ratios being about 2.9 and by XPS measurements. Due to the loose contact between the components in the mechanical mixtures of PdO and Co_3O_4 (11.3 at.% Pd–Co, Fig. 1) Pd as a hydrogen source does not affect significantly the reduction behavior of Co_3O_4. PdO is reduced below ambient, and the decomposition of the hydride phase appears at 353–363 K.

Intimate contact between the Pd and Co phases, achieved by oxidation of the fully reduced samples, modifies the reduction behavior. In the TPR spectra, the reduction peaks appear at 423, 473, and 558 K. A further feature of the TPR data is the absence or limited formation of the Pd hydride phase. Since the intensity of the first reduction peak is proportional to the Pd concentration, we assign this peak to the reduction of Pd^{2+} interacting with Co oxide. Interaction of Pd^{2+} with the Co phase causes an upward shift of 170–180 K in its TPR, whereas the reduction temperature of the Co phase decreases by about 100–120 K. The latter phenomenon is well documented in the literature and is attributed to the enhanced availability of surface hydrogen. In the case of Pd^{2+} the increase in reduction temperature indicates the stabilization of Pd^{2+} by the Co_3O_4 phase. This is likely due to the formation of Pd–O–Co bonds and to the segregation of Co oxide on the surface of PdO particles. The XRD results indicate that even after oxidation at 723 K some metallic Pd is still present.

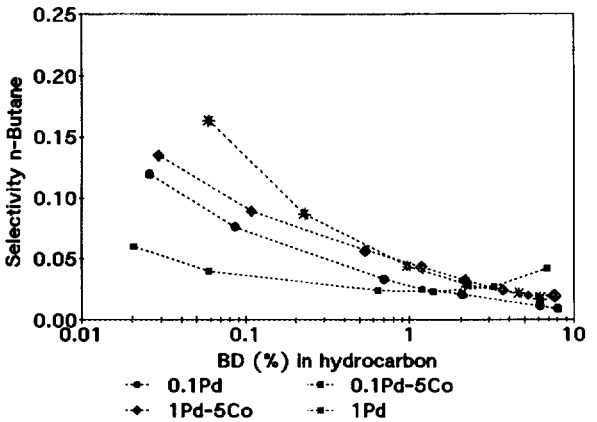

FIG. 13. Selectivity of *n*-butane formation in hydrogenation of 8.9 mol% 1,3-butadiene in 1-butene. (Same reaction conditions and symbols as Fig. 12.)

On the other hand, the XPS technique did not detect Pd^0 on the surface. This can be attributed to the formation of a cherry-type structure with Pd in the center and Co oxide enriched on the surfaces. Restricted hydrogen transport through the Co oxide skin also explains the decreased formation of the hydride phase at room temperature. With a 20 K/min ramp rate, the H/Pd ratio first increases up to about 473 K before decreasing at higher temperatures as presented in Fig. 2. This fact provides additional evidence that the reduction peak at 423 K is connected with the formation of Pd. The decrease in H/Pd ratio above 573 K (with the mechanical mixture the decrease was observed from 623 K) provides evidence for the formation of Pd–Co alloy particles. On the basis of the Pd_{3d}/Co_{2p} peak intensity ratios in Table 3, the surface segregation behavior can be characterized. When both Pd and Co are oxidized, the surface Pd content is significantly lower for both metals than it is in the zero valent state. Repeated reoxidation also decreases the surface Pd concentration. The variation in the Pd/Co signal ratio upon different treatments tracks significant movement of the constituents, i.e., oxidation leads to cobalt surface enhancement while reduction effects Pd enrichment on the surface. The increase in surface Pd concentration is apparently connected with the formation of metallic Co, as indicated by the sharp increase in the Pd/Co ratio in the reduced state of the sample. The overall decrease in surface Pd concentration in the second sequence of treatments (rows 5–9 in Table 3) can be rationalized in two ways: (i) Repeated oxidation and reduction causes mixing of the constituents that leads gradually to a homogeneous sample. (ii) The average particle sizes of the independent Pd- and Co-containing phases change at different rates: Pd may grow more rapidly than the Co particles, which results in a relatively higher dispersion of Co. Whatever the real explanation, the results clearly show

that the contact between Pd and Co phases is much greater after reoxidation of the reduced sample.

The most important changes in the TPR of the Pd–Co/Al_2O_3 samples are associated with the surface Co phase. In agreement with previous results (23–25) reduction of the Co/Al_2O_3 catalysts is significantly affected by the temperature of calcination and the length of time used for drying and decomposing the Co precursor. The presence of Pd on Co/Al_2O_3 decreases the reduction temperature of cobalt and increases the degree of reduction shown by the amount of consumed hydrogen (Table 1). The 5 wt% Co/Al_2O_3 sample treated under O_2 at 623 K can be characterized by the primary reduction peak at 553 K. Oxidation of the once-reduced sample at 623 or 723 K results in a drastic decrease in peak intensity, and the reduction profile becomes similar to those in which the precursor is first oxidized at 723 K. These measurements indicate that the oxidation of the precursor at 623 K leads to an unstable surface structure. Repeated oxidation or calcination at 723 K apparently promotes surface spreading of Co^{2+} and formation of a surface spinel phase $CoAl_2O_4$ (23–25).

Because a considerable part of the CO is in the spinel phase, the Co content of the Pd–Co particles is significantly less than the nominal composition of these catalysts. The metallic ratio of Pd/Co, in view of the reduction results in Table 1, is 0.036, 0.16, and 0.31 for the 0.1Pd–5Co, 0.5Pd–5Co, and 1Pd–5Co samples, respectively. The first TPR peak (Fig. 3) assigned to the reduction of Pd^{2+} shifts gradually to lower temperatures with an increase in the Pd/Co ratio. As demonstrated on the 1Pd–5 Co/Al_2O_3 sample in Fig. 4 (curves 5–8), the peak area connected with Pd^{2+} is not sensitive to repeated oxidation–reduction treatments. The presence of Pd facilitates oxidation of cobalt to Co^{3+}, which might provide an explanation why the Pd–Co system loses less Co by spinel formation in repeated oxidation–reduction treatments than does the Co-only system.

These experimental results suggest a model for the Co–Pd/Al_2O_3 catalysts. In the reduced state the surface consists of Co and Pd–Co ensembles supported on Co spinel. The concentration of separate Pd particles should be low, as indicated by the absence of hydride phase formation. The hydrogen uptake increases with temperature between 273 and 460 K (Fig. 5), which indicates the activated nature of hydrogen chemisorption on separate Co sites. Activated adsorption of H_2 over supported Co is well documented by Zowtiak and Bartholomew (28) and Reuel and Bartholomew (29). We have observed that the desorption temperature of previously adsorbed hydrogen markedly influences the hydrogen uptake. For example, degassing at 723 instead of 573 K largely suppresses hydrogen chemisorption below 373 K. This leads us to attribute the activated nature of H_2 adsorption to the partial oxidation of Co sites by OH groups or by desorbed water. Oxidation of Co sites might explain why the difference in hydrogen uptakes between Co/Al_2O_3 and Pd–Co/Al_2O_3 is the largest at 273 K. The activation energy of adsorption determined by the method of Schwartz (see Refs. 30, 31) has been observed to decrease with Pd, indicating that the redox property of Co and Pd–Co sites is affected by Pd.

The absence of separate Pd particles probably originates from the preparation procedure. During preparation of the Co–Pd/Al_2O_3 catalysts, the dark color of the impregnated precursor indicated that Co^{2+} ions were oxidized to Co^{3+} upon admission of the basic solution of $Pd(NH_3)_2(NO_2)_2$. The oxidation of Co^{2+} is a consequence of the higher stability of Co^{3+} complexes in basic media. The oxidation of Co^{2+} is not accompanied by the reduction of Pd^{2+} (this step might not be expected at pH 9–10; moreover, there was no indication of hydrogen chemisorption on the dried sample) but might facilitate interaction between Co and Pd ions.

Admission of as little as 0.01 at.% Pd to 5 wt% Co/Al_2O_3 significantly increases the hydrogenation activity and influences the product selectivity. First, we consider results presented in Fig. 7 and Table 4. While the 5 wt% Co/Al_2O_3 sample reduced at 573 K showed slight hydrogenation activity at ambient, reasonable activity could only be achieved by reducing the sample at 723 K. It is a feature of these samples that, because of the surface poisoning, the rate of butadiene consumption decelerates. Production of *n*-butane could also be observed, although its formation ceased in repeated experiments. Wells and co-workers performed their hydrogenation experiments between 350 and 390 K. Under those conditions the surface should be heavily poisoned by carbonaceous materials and hence *n*-butane was practically absent. As shown by Tables 4 and Fig. 7, the reduction temperature did not significantly affect the product selectivity over 5 wt% Co/Al_2O_3; with an increase in reduction temperature the selectivity of 1-butene formation decreased but the *trans/cis* ratio of 2-butenes remained nearly constant. On the Pd catalysts the *trans/cis* ratios range between 7 and 12, depending on the preparation and experimental conditions, (32–34). Adsorbed butadiene apparently preserves its σ-*trans* form and the π-allylic bond does not allow free rotation in the half-hydrogenated state (32). With 0.1 and 1 wt% Pd/Al_2O_3, following reduction at 573, we observed *trans/cis* values of 6.8 and 7.3, respectively. Over Pd–Co samples the variation in the *trans/cis* ratio with the reduction temperature reflects the formation of Pd–Co and Co sites. Reduction at ambient gave *trans/cis* ratios of 3–5, which indicates that Pd sites are working even though the observed *trans/cis* ratio is smaller than on Pd/Al_2O_3. The increase in *cis* isomer may be tentatively attributed to the cooperation of Co^{3+} or Co^{2+} sites. As shown in Fig. 7, most of the selectivity changes appear between 298 and 473 K. Above 473 K the *trans/cis* ratio reaches values in the range of 2.5–3 and

Table 5

Hydrogenation Rates of 1,3-Butadiene and Butene Intermediates

Exp	1Pd	5Co–1Pd	5Co–0.5Pd	5Co–0.1Pd	5Co	0.1Pd
A	0.46–0.49	0.64–0.71	1.12–1.38	1.65–1.93	—	—
B	0.51	0.49	0.47	3.11	—	—
TOF[a]	0.92	0.94	0.92	0.23	0.1	1.0
TOF[b]	1.5	1.56	1.59	0.23	0.1	0.9

Note. A (298 K) and B (313 K) represent rate ratios ($-R_{BD}/R_{nB}$) of initial 1,3-butadiene consumption divided by initial *n*-butane formation *after* all the 1,3-butadiene disappeared. The range given for A represents multiple experiments. For the 5 wt% Co/Al_2O_3 (penultimate column) the ratios are 3.5 and 23 at 423 and 353 K, respectively; reactants are 1.33 kPa butadiene and 5.32 kPa hydrogen. TOF (sec^{-1}) (1.33 kPa butadiene, $H_2/BD = 2$).

[a] Calculated from maximum H_2 uptake.

[b] Calculated from irreversible CO adsorption.

slowly decreases upon prolonged reduction. It should be noted that while the selectivity values show only a small decrease, the rate of butadiene consumption increases significantly between 473 and 723 K. We attribute this result to the formation of Pd–Co and Co ensembles rather than to the separate action of Pd and Co sites. The latter implies a constant ratio of Co and Pd sites with increased reduction temperature, which is not likely. Even though the decrease in surface Co (see Table 3) implies that Pd segregates on the surface, this increase in Pd concentration is not reflected in the *trans/cis* ratio. Recent compositional studies (35) on oriented single crystal [111] and [100] surfaces of the alloy $CoPt_3$ have shown that the outermost atomic layer is essentially Pt with a second layer enriched in Co. On these surfaces there is a substantial decrease in the CO desorption activation energy in comparison with pure Pt, indicating a change in the electronic state of the Pt. A similar electronic effect may explain the ability of zerovalent chromium to decrease the hydrogenolysis activity of Pt–Cr clusters (36–38). The variation in the strength of diene and alkene complexation is clearly indicated by the $-R_{BD}/R_{nB}$ ratios (Table 5). At decreased Pd concentrations the rate of alkene hydrogenation is suppressed to a larger extent than is the reaction of the diene. The rapid decrease in the 1-butene selectivity during measurements with 1-butene and 1,3-butadiene mixtures indicates an enhanced isomerization activity of the sample. Although *n*-butane is formed continuously, the consumption of 1-butene is not primarily the result of full hydrogenation. To explain the above observations one might tentatively consider (i) electronic interaction between Pd and Co, or (ii) poisoning of Pd–Co clusters by the retention of hydrocarbons on Co sites. The latter argument is supported by the rapid initial poisoning of pure Co and by the decrease in TOF with the decrease in Pd concentration.

In summary, the Pd–Co system we have investigated, electronic and poisoning effects cannot be clearly separated from effects due to the presence of Pd–Co and Co sites that act simultaneously in hydrogenation.

CONCLUSIONS

1. The presence of 0.1, 0.05, and 0.01 at.% Pd in 5 wt% Co/Al_2O_3 increases the reducibility of Co and the number of metallic centers.

2. The experimental results suggest the simultaneous presence of a surface Co phase (surface aluminate), Co, and Pd–Co bimetallic particles. Adsorption curves recorded under 0.13% H_2/Ar confirmed activated adsorption of hydrogen.

3. With an increasing Co/Pd ratio, the rate of *n*-butane formation is suppressed to a greater extent than is the consumption of 1,3-butadiene. These results also indicate an enhanced isomerization activity of 1-butene. Accompanying these effects is a decrease in the TOF values that points to significant electronic interactions between Pd and Co and/or poisoning of separate Co sites.

ACKNOWLEDGMENTS

The authors are indebted to Mr. P. Y. D. Leflaive for his assistance in the XPS measurements. The financial support of the Hungarian–American Joint Fund (Grant J-183) and COST Program (D5/01/93) is greatly acknowledged.

REFERENCES

1. Boitiaux, J. P., Cosyns, J., Derrien, M., and Leger, G., *Hydrocarbon Process.* **64,** 51 (1985).
2. Derrien, M., *in* "Studies in Surface Science and Catalysis" (L. Cerveny, Ed.), Vol. 27, p. 613. Elsevier, Amsterdam, 1986.
3. Guczi, L., and Schay, Z., *in* "Studies in Surface Science and Catalysis" (L. Cerveny, Ed.), Vol. 27, p. 313. Elsevier, Amsterdam, 1986.
4. Lindlar, H., *Helv. Chim. Acta* **35,** 446 (1952).
5. Cerveny, L., Paseka, I., Surma, K., Thanh, N. T., and Ruzicska, V., *Collect. Czech. Chem. Commun.* **50,** 61 (1985).
6. Travers, C., Bournonville, J. P., and Martino, G., *in* "Proceedings, 8th International Congress on Catalysis, Berlin, 1984" (G. Ertl, *et al.*, Eds.) Vol. 4, p. 891. Dechema, Frankfurt-am-Main, 1984.
7. Mallat, T., Szabo, S., and Petro, J., *Appl. Catal.* **29,** 117 (1987).
8. Palczewska, W., Ratajczikowa, I., Szymrska, I., and Krawczyk, M., *in* "Proceedings, 8th International Congress on Catalysis, Berlin, 1984" (G. Ertl *et al.*, Eds.) Vol. 4, p. 173. Dechema, Frankfurt-am-Main, 1984.
9. Palczewska, W., Jablonsky, A., Kuszkur, Z., Zuba, G., and Warnish, J., *J. Mol. Catal.* **25,** 307 (1984).
10. Borgna, A., Moraweck, B., Massardier, J., and Renuprez, A. J., *J. Catal.* **128,** 99 (1991).
11. Aduriz, H. R., Bodnariuk, P., Coq, B., and Figueras, F., *J. Catal.* **129,** 47 (1991).
12. Furlong, B., Hightower, J. W., Chan, T.Y-L., Sarkany, A., and Guczi, L., *Appl. Catal. A. General,* **117,** 41 (1994).
13. Ponec, V., *Catal. Rev. Sci. Eng.* **11,** 1 (1975).

14. Sinfelt, J. H., "Bimetallic Catalysis: Discoveries, Concepts and Applications." Wiley, New York, 1983.
15. Lahtien, J., Anraku, T., and Somorjai, G. A., *J. Catal.* **142,** 206 (1993).
16. Iglesia, E., Soled, S. L., Fiato, R. A., and Via, G. H., *J. Catal.* **143,** 345 (1993).
17. Zsoldos, Z., Hoffer, T., and Guczi, L., *J. Phys. Chem.* **95,** 798 (1991).
18. Guczi, L., Hoffer, T., Zsoldos, Z., Zyade, S., Maire, G., and Garin, F. J., *J. Phys. Chem.* **95,** 802 (1991).
19. Zsoldos, Z., and Guczi, L., *J. Phys. Chem.* **96,** 9393 (1992).
20. Phillipson, J. J., Wells, P. B., and Wilson, G. R., *J. Chem. Soc. A,* 1351 (1969).
21. Oliver, R. G., Wells, P. B., and Grant, J., *in* "Proceedings, 5th International Congress on Catalysis, Palm Beach, 1972" (J. W. Hightower, Ed.), Vol. 1, p. 659. North-Holland, Amsterdam, 1973.
22. George, M., Moyes, R. B., Ramanarao, D., and Wells, P. B., *J. Catal.* **52,** 486 (1978).
23. LoJacono, M., Schiavello, M., and Cimino, A., *J. Phys. Chem.* **75,** 1044 (1971).
24. Chin, R. L., and Hercules, D. M., *J. Catal.* **74,** 121 (1982).
25. Arnoldy, P., and Moulijn, J. A., *J. Catal.* **93,** 38 (1985).
26. Hightower, J. W., Furlong, B., Sarkany, A., and Guczi, L., *in* "Proceedings, 10th International Congress on Catalysis, Budapest, 1992" (L. Guczi, F. Solymosi, and P. Tetenyi, Eds.), Vol. 3, p. 2305. Adkadémiai Kiadó, Budapest, 1993.
27. Sarkany, A., Zsoldos, Z., Furlong, B., Hightower, J. W., and Guczi, L., *J. Catal.* **141,** 566 (1993).
28. Zowtiak, J. M., and Bartholomew, C. H., *J. Catal.* **83,** 107 (1983).
29. Reuel, R. C., and Bartholomew, C. H., *J. Catal.* **85,** 63 (1984).
30. Falconer, J. L., and Schwarz, J. A., *Catal. Rev. Sci. Eng.* **25,** 141 (1983).
31. Lee, P. I., and Schwarz, J. A., *J. Catal.* **73,** 272 (1982).
32. Bond, G. C., and Wells, P. B., *Adv. Catal.* **15,** 91 (1964).
33. Meyer, E. F., and Burwell, R. L., *J. Am. Chem. Soc.* **85,** 2281 (1963).
34. Boitiaux, J. P., Cosins, J., and Robert, E., *Appl. Catal.* **35,** 193 (1987).
35. Bardi, U., Beard, B. C., and Ross, P. N., *J. Catal.* **124,** 22 (1990).
36. Joyner, R. W., Shpiro, E. S., Johnston, P., and Tuleuova, G. J., *J. Catal.* **141,** 250 (1993).
37. Shpiro, E. F., Joyner, R. W., Johnston, P., and Tuleuova, G. J., *J. Catal.* **141,** 266 (1993).
38. Joyner, R. W., and Shpiro, E. S., *Catal. Lett.* **9,** 239 (1991).